G.R.E.EN.

General Relativistic Effects on ENtanglement

Summer School Alpbach 2015

July 23rd, 2015

Team Green: Simon Coop, Maciej Jakubczak, Jukka-Pekka Kaikkonen, Paul Knott, Jonathan Kolbeck, Laura LeBarbier, Jessica McKenna, Virginia Notaro, Franck Octau, Jone Peter Reistad, José Rocha, Filip Rozpedek, Constantin Weisser, Robert Wenger, Parisa Yadranjee Aghdam

Team Green would like to thank FFG, ESA, ISSI, and Austrospace for organizing the Summer School Alpbach 2015. Also thanks to all the tutors and lecturers guiding team Green towards this product, and a special thank to our team tutors David Fischer and Carsten Scharlemann. For financial support for attending the Summer School, we thank SNSB, NSC, DLR, ASI, CMNP, CNES, ULP, UKSA, WUT FP, SRON, TU DELFT, Luofona University of Porto

Abstract

The theories of General Relativity (GR) and Quantum Mechanics (QM) form the basis of our current understanding of the universe. In spite of their individual experimental successes, there are great conceptual conflicts between the current formulations of QM and GR. Up to now a complete theory of quantum gravity that reconciles these conflicts has eluded scientists. Since no such theory has yet provided satisfactory unification, GREEN will probe the domain of the intersection of these two theories. With the possibility of producing results that conflict with either QM or GR, or perhaps both, GREEN aims to provide new evidence to aid the development of emerging theories of quantum gravity. This will be achieved by measuring a general relativistic effect on a quantum system - more specifically a gravitational redshift induced on entangled photons. GREEN employs a satellite in an elliptical orbit around Earth sending entangled photons to a ground station. Firstly, decoherence due to the large separation or gravitational potential difference will be investigated by performing a Bell test. Secondly, by utilizing the large gravitational potential difference between ground and space, together with state of the art technology, we will be able to detect any differences down to 1 % from the classical gravitational redshift value for the entangled photons. The impact of our result will provide further knowledge on the validity of QM and GR, and possibly trigger further development of a unifying theory.

1. Introduction

1.1 Two Revolutionary Theories

In the beginning of the 20th century two physical theories emerged that sparked a revolution in physics and greatly advanced our understanding of the universe.
The first of these theories was Einstein's 1916 theory of general relativity (GR), a classical theory of gravitation arising from the extension of special relativity to curved spacetime. It is characterized typically by massive bodies and cosmological length scales.
The second of these two theories is quantum theory (QM) which is typically characterized by atomic or sub-atomic length scales.
The predictions of both QM and GR have since been experimentally verified in their respective domains.

1.2 The Clash

In spite of their respective successes, there remains a huge problem in reconciling QM and GR. Some of the conflicting concepts of the two theories are compared below.

Table 1

General Relativity	Quantum Mechanics
Spatial nonseparability (non-locality) is implied by the superposition principle	GR asserts complete spatial separability (locality)
Equivalence Principle	Uncertainty Principle
Time as a dimension	Time as a parameter

QM does not obey the principle of local realism. This means that for a quantum system can display entanglement – so two photons can exhibit correlations even when spatially separated. Einstein called this 'spooky action at a distance' – the states appear to be able to communicate, or to be somehow governed by each other. This is contrary to the theory of GR, obeying local realism, which states that any particle is only affected by its immediate surroundings. GR is a spatially separable geometrical phenomenon.

It's clear that the current formulations of QM and GR are irreconcilable – our understanding is incomplete. But where exactly do the inconsistencies lie? – This is the question that motivates the GREEN mission.

1.3 In the Space Laboratory - Gravitationally induced redshift

As light escapes a region of high gravitational potential it loses energy and appears shifted towards the red end of the electromagnetic spectrum, exhibiting a lengthened wavelength. This prediction of GR was successfully confirmed for classical light by Gravity Probe A [1].
This has not been demonstrated for entangled quantum states.

2. Proposed experiment

2.1 Testing Fundamental Physics - Why Space?

One of the biggest challenges in exploring the valid regimes of the two theories is the fact that GR requires large distances and mass densities to be detectable.

Hence, exposing a quantum system to an environment governed by GR effects is practically very challenging. Since observations on the ground are limited to relatively small distances (the record distance over which an entangled state has been sent stands at 144km) and nearly uniform gravitational potentials, space is a natural laboratory for such experiments.

2.2 Outline

In this experiment, entangled photons created by a source in space are separated spatially by sending one to Earth (see Figure 1). By performing a Bell test on the ground and satellite we will be able to determine the effect on entanglement of:

- The long Earth-satellite distance
- The Earth-satellite gravitational potential

There are no laws in QM that put bounds on the distance over which entanglement can exist, nonetheless the result of our Bell test will in itself be an important result as this has not yet been shown to hold over distances larger than 144 km[2].

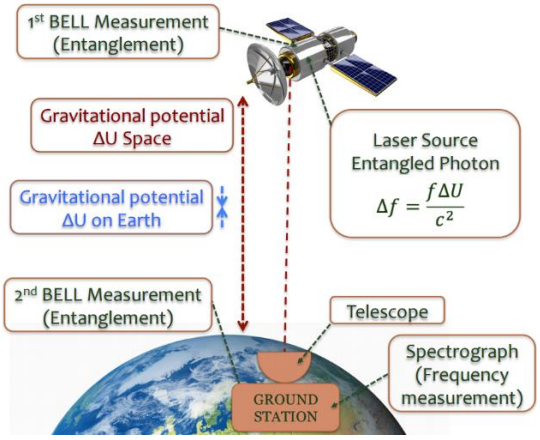

Figure 1

Since a positive result of the Bell test is expected (entanglement is present), it would be of great interest to know if the entangled photon that experienced the gravitational potential ΔU also is red shifted, since its highly correlated partner has not experienced the ΔU.
By measuring the frequency of the entangled photon on the ground we can identify the red shift experienced and compare it to the corresponding value for the redshift of classical photons. In doing this, GREEN is expected to produce results that clash in some way with our current formulations of GR or QM.
If the experiment shows that the red shift is different from its classical value, GR in its present state cannot be true, which has never been proven before.

This will help scientist further constrain QM in the search for a unified theory of QM and gravity.

3. Scientific objectives and requirements

Table 2

Science Objective	Science Requirements
SO1: Explore the role of gravity on quantum entanglement	**SR1.1:** Separate entangled photons over a gravitational potential of 107J/kg **SR1.2**: Determine if entanglement still is present after photon has experienced a gravitational potential change. This needs to be confirmed with 99.7% confidence by testing Bells inequality over a large range of different distances
SO2: Investigate the effect of large spatial separations on quantum entanglement	**SR2:** In addition to SR1, provide distances from 500 km to 10 000 km between the entangled photons.
SO3: Search for hints of discrepancies between QM and GR by comparing the gravitational red shift of entangled photons with the expected red shift from classical photons	**SR3:** Determine the gravitational red shift of the entangled photons with precision of 1% of the classical value

4. Instrument requirements

4.1 Gravitational redshift

We are limited by the gravitational potential difference ΔU between our orbit and the ground. For a given frequency f this translates into a gravitational redshift $\Delta f = \frac{f\Delta U}{c^2}$. The figure shows how the redshift value for the entangled photons varies as a function of altitude. One can see that only redshifts of up to 100 KHz is possible within Earth's gravitational field.

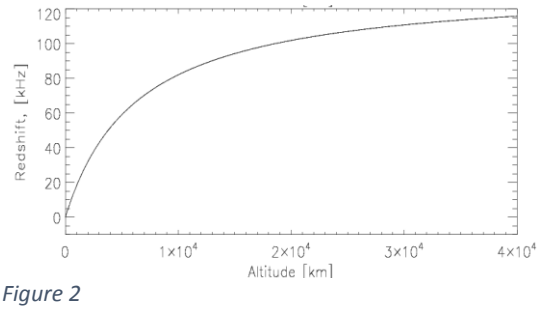

Figure 2

4.2 Orbit

Due to systematic uncertainties from sources on the satellite and on the ground, absolute values of the gravitational redshift are difficult to measure.

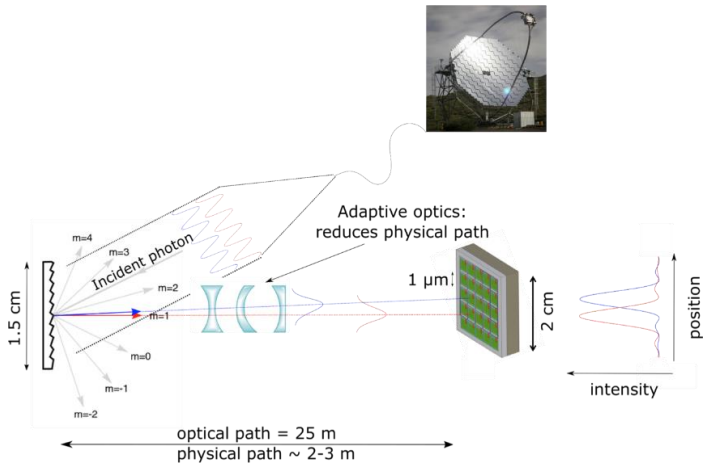

Figure 3

An elliptical orbit was chosen, so that a variation in frequency could be observed. Measurements are collected in 25 sections in eclipse around the perigee and apogee to avoid radiation damage to the detectors when passing through the Van Allen belt.

In each section the deviations of the entangled photon from a classical photon is averaged. This corresponds to one data point on a graph of Δf against the gravitational potential.

4.3 Limitations from photon source

The resolution of the frequency measurement is determined by the bandwidth of the photons, hence the narrowest bandwidth photon source is used. A nonlinear silicon nitride crystal microring resonator source with a continuous wave (CW) pump [2] was chosen to produce entangled photons with low bandwidth of 30 MHz [1] at 1550 nm wavelength.

To resolve the frequency to 1% of the classical value, 10^9 observations are needed. A disadvantage of this source is however the modest pulse rate of 50 Mcps, hence it's paramount that signal attenuation be minimized A schematic of the optical system is given in the figure below.

4.4 Spectrometer

It's desirous to have measuring apparatus with accuracy of the same order of magnitude as the photon bandwidth in order to measure the frequency of the photons to accuracy $\Delta f_a = 10\ MHz$

This is more advanced than any spectrometer commercially available at this time. The accuracy of the single measurement is: $\Delta f_s = 10\sqrt{10}\ MHz$

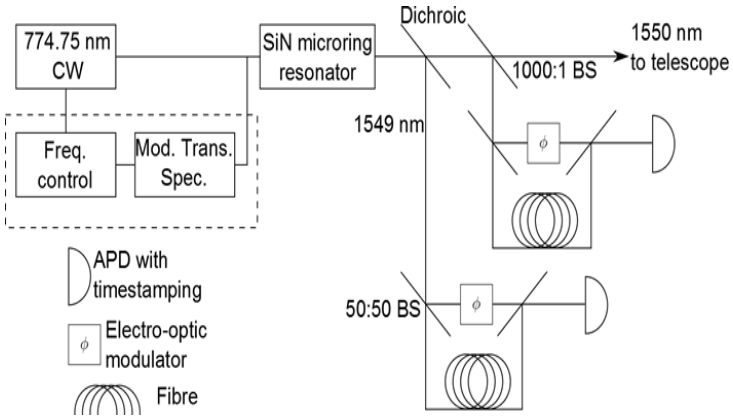

Figure 4 Satellite Optics

It is sufficient to use a diffraction grating and to reconstruct the intensity pattern around the first order maximum to determine the wavelength of light. Using a blazed grating, the intensity of the first order maximum is 80% of the total incident light.

An array with length of 2 cm and pixel size of 1 μm is required. This setup also requires a 25 m long optical path between the grating and the detector array. However, this optical path will be reduced to ~2 to 3m using adaptative optics.

In the spectrometer SPADs (single photon avalanche diode) are used for the frequency measurement of each photon. The quality of SPAD is characterised by its Dark Count Rate (DCR). GREEN employs SPADs with DCR 100 cps operating at 193K to ensure photon Detection Efficiency of 10%.

4.5 Satellite Telescope

The telescope employed on the satellite is very similar to the LISA telescope [3] with mechanical length 60 cm and 50 cm of aperture with a magnification power of 100.
The estimated mass is 20 kg. A pointing accuracy of 5 μradians is required in order to detect the laser beam on Earth.

4.6 Ground Telescope

The proposed ground station is the Magic Telescope, on Canary Islands, with a diameter of 17 meters. This telescope is able to point to any direction in the sky within 40 seconds and also have a adaptive optics device for aberration compensation.

4.7 Optical link budget

The instrument requirement is mainly limited by the photon rate. To obtain 1KHz accuracy, the mission shall provide at least 10^9measurements. From figure 5 it can be seen that losses amount to 40dB. This includes atmospheric losses, diverging beam, telescope losses, grating losses and the spectrograph with detectors.

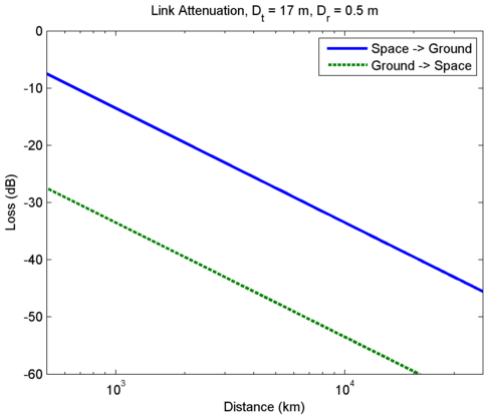

Figure 5 Optical Losses

4.8 Instrumentation: Bell Test

The Bell test is a routine statistical test used in quantum mechanics to determine whether two particles are entangled.
The minimum signal-to-noise ratio (SNR) required to prove the presence of entanglement in the Bell test is ~4.8

InGaAs/InP single-photon avalanche diodes (SPAD) were chosen for both ground and satellite since low dark count and fast detection rates are required. MZIs have to be also temperature controlled to avoid fluctuations in the path-length difference.
SNR > 4.8 required for the Bell test is satisfied. An on-board Bell test is also performed to one in 1000 photons (see Fig. 'opt schematic'). The violation of Bell inequalities is within confidence level of three standard deviations.

Photon pair production rate, *P* (MHz)	50
Ground detector efficiency, η	0.7
Link efficiency, (dB)	-40
Coincidence window (ns)	~ 1
Dark count rate (kcps)	100
Background (kcps)	10

4.9 Error Analysis

The Doppler shift, for example, modifies the signal as in the figure below. The blue line is the expected measurement of the frequency shift of a photon with a reduced Doppler shift for illustration.

Only the deviation of the frequency shift from that of a classical photon will be determined and calibration

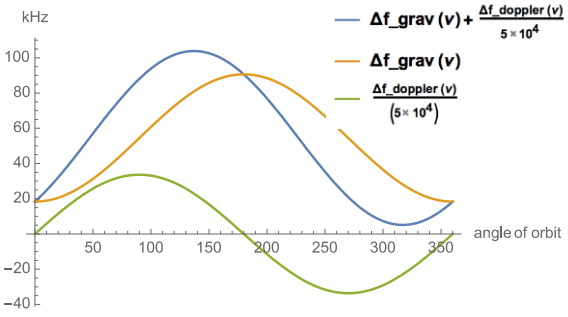

Figure 6

methods are adopted. For the calibration procedure, measurements will be performed on quantum and classical photons.

Source	Size of Error	Remedy	After Remedy
Doppler shift	10^5 bigger than original signal	6 cm orbit precision	<1% on each data point
Stability of laser	10 MHz	Frequency Stabilisation 1kHz	$<10^{-6}$ %
Spectrometer Dark Count, Satellite Black Body Radiation	10^6 counts per seconds	Cooling and Temperature Stability	100 counts per second
Averaging over photons of different gravitational potentials	<1kHz	None	$<10^{-6}$ %
Systematic errors	Any size	Classical Photon Measurement	0

4.10 Timing

During measurement time the same 60 second procedure as shown in figure (7) is followed repeatedly.

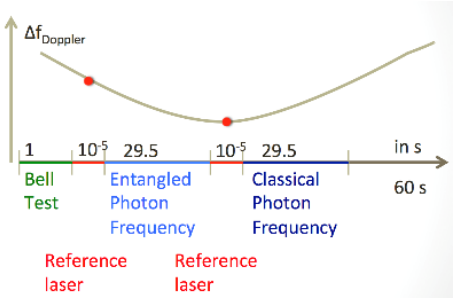

Figure 7 Measurement Timing

5. Mission profile

5.1 Spacecraft design

The spacecraft needs to be stiff to avoid any structural deformations that could interfere with the measurement and also has to resist to the launch loads.
Therefore, the payload is stored inside a central cylindrical structure, that is connected to the outer structure by shear panels. This configuration provides a direct path for the design loads to be redistributed through the geometry. Both the solar panels and the antenna need gimballing.

Material Characteristic	Value
Longitudinal Young Modulus (GPa)	181
Transversal Young Modulus (GPa)	10.3
Density (Kg/m^3)	1600
Thermal expansion coefficient (K^{-1})	$-1*10^{-6}$

CFRP (Carbon Fiber Reinforced Plastic) was chosen as a structural material for its high Young's modulus, low density and low thermal deformation.

5.2 Thermal subsystem

The payload & subsystems require high thermal stability and a low temperature (0° C).

The spacecraft has both a passive and an active thermal control system to keep both the payload and the subsystems in their proper temperature range. For the payload, Peltier cells and a heat pipe device are used to provide local thermal stability. Due to blackbody radiation the temperature requirement is $T < 220K$ for performing measurements.The 2-axis gimballing mechanism assures that both the solar panels and the antenna are in the correct position when the spacecraft enters the eclipse part of the orbit. Any reflected radiation could indeed affect the measurements.

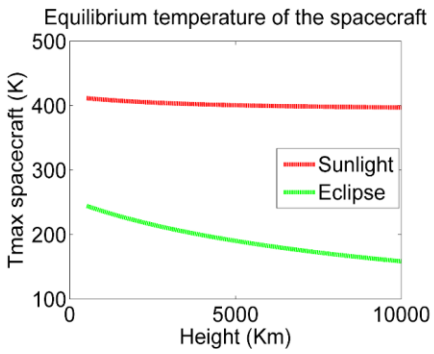

Figure 8

5.3 Power subsystem

The power required during sunlight is approximately 1.2 kW. Triple-junction GaAs solar cells that can provide (with an efficiency of 0.25) 238 w/m^2 EOL are chosen. Progressive degradation of the solid state cells was taken into account when designing the total area of the solar array. Also, during sunlight the solar arrays have to provide enough energy to charge the batteries; the resulting total area is 7m^2. For the batteries, Nickel-Hydrogen cells were chosen. They have a voltage of 2.5 V (per cell), a mass efficiency of 70 Wh/kg and a Depth of Discharge of 0.7. In order to provide sufficient energy to power the measuring instruments, they are required to have a total capacity of 1.9 kWh BOL, and are packed in arrays located in the bottom module of the spacecraft.

5.4 Attitude and Orbit Control Subsystem

To have a successful measurement, the optical axis of the telescope must be inside a cone with an aperture of 5 microradians (1 arcsecond). This is achieved by means of a precise attitude determination and control system. Two star sensor are used to determine (within 1 arcsecond) the spacecraft's attitude and to calibrate a Ring Laser Gyro, which will measure angular velocity with a precision of 0.01 deg/hour. The optimal way to rotate the satellite when it enters and exits the eclipse zone and to balance disturbance torques is to use 4 reaction wheels (1 per axis and 1 for redundancy) and 12 Reaction Control Thrusters (also doubled for redundancy). The RCS system's function is to desaturate the wheels when they reach their limiting angular momentum value, and also to win the strong atmospheric drag resistance throughout the 3-year lifetime.

A guidance laser retroreflector is also used to improve the knowledge of both the orbit and the spacecraft's attitude.

5.5 Propulsion Subsystem

There was a trade-off between chemical and electrical propulsion. The former requires less power but a total propellant mass (including atmospheric drag reaction, station keeping, debris avoidance maneuvers and final deorbiting burn) of 302 Kg, while the latter requires a very little amount of mass, but much more power.

Since power is a critical driver for this mission, the chosen propulsion system is the chemical one; it will use *ADN green propellant* with a specific impulse of 255 s.

Delta V Budget	
Orbit Corrections	75m/s
East-West Stationkeeping	6m/s
North-South Stationkeeping	55m/s
Survivability (incl. Ev. Maneuvers)	200m/s
Drag-Makeup	200m/s
Controlled Reentry	150m/s
Total Delta V:	686m/s
Amount of RCS Thrusters:	12

Figure 9

5.6 Orbit description

Inclination	27.7
Orbit	500km to 10,000km
Eclipse time Apogee	60 min

Eclipse time Perigee	< 30 min
Total eclipse time	~4 h / day
Orbit Period:	3.5 h

5.7 Communication

For communication between the satellite and the ground station two different RF-links are used. First, for the housekeeping data, a channel over S-Band is chosen. For the measurement data, which must have a higher data rate, a second channel over X-Band is provided. For command communication and tracking of the entanglement of the produced photons on the satellite, the link should also be available at the start and during measurement in apogee.

	S-Band (Apogee)	**S-Band (Perigee)**	**X-Band (Perigee)**
Distance	10 000 km	500 km	500 km
Power	5 W	5 W	20 W
Dish diameter on SAT	50 cm	50 cm	50 cm
Antenna diameter on GS	13 cm	13 cm	13 cm
Frequency	2 GHz	2 GHz	10 GHz
Transmission loss (LS+La)	-180.7 dB	-154.7dB	-168.6 dB
EIRP	12.6 dB	12.6 dB	32.6 dB
Rx G/T	-6.4 dB	-6.4 dB	7.5 dB
EB/EN	20.8 dB	46.8 dB	30.1 dB
Data rate	2 kbps	2 kbps	10 Mbps

5.8 Power and mass budget

The payload represents approximately 14 % of the total satellite mass. The column on the right side shows the mass of the subsystems with a 25% margin. A 40% margin was added to the total satellite wet mass.

Subsystem	Power consumption	Mass (w/o margin)	Mass (w/ margin)
Propulsion system	100.0W	75.2kg	94.0kg
AOCS	100.0W	63.0kg	78.8kg
TCS	200.0W	53.6kg	67.0kg
OBDH	25.0W	21.0kg	26.3kg
TT&C	25.0W	35.0kg	43.8kg
Structure and mech.	50.0W	168.8kg	211.0kg
EPS	100W	165.0kg	206.3kg
Payload	300.0W	150.0kg	187.5kg
Launch adapter		150.0kg	150.0kg
Satellite (dry mass)	800.0W	881.6kg	1064.5kg
Propellant (ADN)		512.0kg	640.0kg
Satellite (wet mass)	800.0W	1393.6kg	1704.5kg
Margin (+40%)	1120.0W	1951.1kg	2386.3kg

Figure 10

5.9 Risk Analysis

What?	Consequence	Probability	Severity	Overall Risk
Spectrograph unavailable	Unable to measure Redshift	4	5	20
Entangled Photon Source (Laser)	Delay in the development schedule	3	3	9
Single Photon Avalanche Source (SAPD)	Delay in the development schedule	3	3	9
Interferometer	Delay in the development schedule	3	3	9

Figure 11 Development Risks

What?	Consequence	Probability	Severity	Overall Risk
Deterioration of optical components (e.g. radiation)	Inability to verify entanglement	2	5	10
Solar Flares	Damage to critical components	2	5	10
Continuity of Funding	Mission Delay	3	4	12
Personnel Unavailability	Mission Delay	3	4	12

Figure 12 Mission Risks

5.10 Mission Development Costs

#	Item	Cost (M€)
1	Project Team	45
2	Industrial Cost	350
3	Mission Operations	50
4	Science Operations	40
5	Payload**	300
6	Launcher (Soyuz)	75
7	Contingency	75
	Total:	935

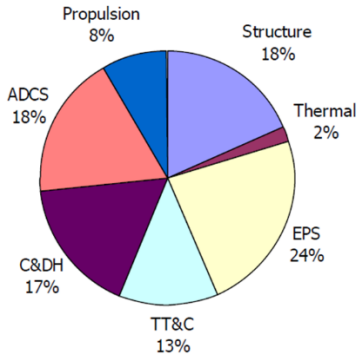

Figure 13

5.11 Descoping options

Our main descoping option is to conduct the measurement of the coherence of entangled photons but not the redshift test. This option will reduce the costs of the mission but not will influence the satellite. Another option could be use a different ground telescope, a smaller one. This is an option that could reduce costs of the ground telescope but the mission lifetime would increase (increased observation time would be necessary

6. Conclusion

The purpose of the GREEN mission is to experimentally test systems at the intersection of the domains of quantum mechanics and general relativity. An insight into the gravitational redshift of entangled photons might either suggest revisions of quantum mechanics or general relativity or restrict predictions of future theories.

References

[1]Technical Details - Gravity Probe A". Nasa JPL. May 2, 2009.
J.F. Clauser, M.A. Horne, A. Shimony, R.A. Holt (1969), "Proposed experiment to test local hidden-variable theories", *Phys. Rev. Lett.* **23** (15): 880–4,Bibcode:1969PhRvL..23..880C, doi:10.1103/PhysRevLett.23.880
[2]R. Ursin et. al., Nature Phys. 3, pp. 481 - 486 (2007), *Entanglement-based quantum communication over 144 km*
Rupert Ursin, T Scheidl, E Wille; Quantum optics experiments using the International Space Station: a proposal; New Journal of Physics 15 (2013)
[3]K. Danzmann et al., LISA Assessment Study Report, ESA /SRE(2011)3
F. Acerbi, M. Anti, A. Tosi, F. Zappa, *Design Criteria for InGaAs/InP Single-Photon Avalanche Diode*, IEEE Photonics Journal, Vol. 5, No. 2, April 2013.
J. Zhang, M. A Itzler, H. Zbinden and J.-W. Pan, *Advances in InGaAs/InP single-photon detector systems for quantum communication*, Light: Science & Applications (2015) 4.
Dyson, F. W.; Eddington, A. S.; Davidson C. (1920). "A determination of the deflection of light by the Sun's gravitational field, from observations made at the total eclipse of 29 May 1919". *Philosophical Transactions of the Royal Society* **220A**: 291–333.Pound, R. V. et al. (1960). "Apparent weight of photons". *Physical Review Letters* **4** (7): 337–341.Alain Aspect, Philippe Grangier, Gérard Roger (1982), "Experimental Realization of Einstein-Podolsky-Rosen-Bohm Gedankenexperiment: A New Violation of Bell's Inequalities", *Phys. Rev. Lett.* **49** (2): 91–4"Fundamental Physics of Space –